nature materials

LETTERS

PUBLISHED ONLINE: 13 NOVEMBER 2011 | DOI: 10.1038/NMAT3172

Induction of coherent magnetization switching in a few atomic layers of FeCo using voltage pulses

Yoichi Shiota[1], Takayuki Nozaki[1,2†], Frédéric Bonell[1], Shinichi Murakami[1,2], Teruya Shinjo[1] and Yoshishige Suzuki[1,2*]

The magnetization direction of a metallic magnet has generally been controlled by a magnetic field or by spin-current injection into nanosized magnetic cells[1,2]. Both these methods use an electric current to control the magnetization direction; therefore, they are energy consuming. Magnetization control using an electric field[3] is considered desirable because of its expected ultra-low power consumption and coherent behaviour. Previous experimental approaches towards achieving voltage control of magnetization switching have used single ferromagnetic layers with and without piezoelectric materials, ferromagnetic semiconductors, multiferroic materials, and their hybrid systems[4–15]. However, the coherent control of magnetization using voltage signals has not thus far been realized. Also, bistable magnetization switching (which is essential in information storage) possesses intrinsic difficulties because an electric field does not break time-reversal symmetry. Here, we demonstrate a coherent precessional magnetization switching using electric field pulses in nanoscale magnetic cells with a few atomic FeCo (001) epitaxial layers adjacent to a MgO barrier. Furthermore, we demonstrate the realization of bistable toggle switching using the coherent precessions. The estimated power consumption for single switching in the ideal equivalent switching circuit can be of the order of $10^4 k_B T$, suggesting a reduction factor of 1/500 when compared with that of the spin-current-injection switching process.

Recent studies on the voltage control of the magnetic properties of nanosized magnetic cells have attracted considerable attention for their relevance to voltage-driven spintronics applications with low power consumption. These include studies on surface magnetic anisotropy or phase changes in thin ferromagnetic metal films[4–8], magnetoelastic coupling in ferromagnetic/piezoelectric hybrids[9,10], magnetization control in ferromagnetic semiconductors[11–13] and magnetoelectric coupling in multiferroics[14,15]. Most studies so far have been carried out only at low temperatures using GaMnAs or perovskite systems; further, many of these studies have required piezoelectric distortions that may limit the endurance of any device used in the process. In contrast, 3*d* transition metals such as Fe and Co have very high Curie temperatures and show extremely long endurance; these properties are used in magnetic random access memory (M-RAM) applications. Therefore, the voltage control of perpendicular magnetic anisotropy (PMA) in ultrathin ferromagnetic metal films[5,6,16–20] embedded in conventional magnetic tunnel junctions (MTJs; refs 21,22) using a MgO barrier[23,24] has attracted considerable interest.

An important and basic issue that remains to be addressed for practical technological use is the realization of two-way switching between bistable states (P and Q) using just a voltage. As an electric field has time-reversal symmetry, it cannot change the relative depth of the potential wells at P and Q; this is in contrast to the changes that can be achieved in the barrier height between them. Therefore, to obtain one-way switching from P to Q, it is necessary to apply a small assisting magnetic field to change the relative depth of the wells. The reverse switching (from Q to P) requires a magnetic field in the opposite direction; such field-assisted switching has been experimentally demonstrated in other studies[12,16]. To overcome the problem, two methods have been proposed. The first method uses successive anisotropic changes along the different axes[25]; however, the practical application of this method to nanoscale magnetic cells is difficult. The second method uses a high-speed voltage pulse with an asymmetric shape[6] and/or a definite pulse length. In this study, we report the first observations of coherent magnetization switching induced by the application of pulse voltages under a constant-bias magnetic field.

A fully epitaxial (001) oriented MTJ structure comprising a MgO(001) substrate/MgO (10 nm)/Cr (10 nm)/Au (50 nm)/$Fe_{80}Co_{20}$(0.70 nm)/MgO (1.5 nm)/Fe (10 nm)/Au (5 nm) was deposited using molecular beam epitaxy. The film was patterned into a nanopillar with a rectangular cross-section of $800 \times 200\ nm^2$ using electron-beam lithography and an Ar ion-milling technique. The longer side of the rectangular cell was designed to be parallel to the FeCo [100] alignment direction. The resistance–area product in the parallel (P) state and the magnetoresistance (MR) ratio were $56\ \Omega\ \mu m^2$ and 16%, respectively. The bottom ultrathin FeCo layer acts as a magnetically free layer (whose magnetic anisotropy can be controlled by the application of a suitable bias voltage), whereas the top thick Fe layer acts as a magnetically fixed layer. A positive bias voltage is defined as a positive voltage at the top electrode with respect to the bottom electrode. All experiments were performed at room temperature.

Figure 1a shows a MR curve measured under a perpendicular magnetic field. Both ferromagnetic layers exhibit in-plane magnetizations along the length of the cell. As these magnetizations couple in the anti-parallel (AP) state at the remanent state because of the magnetic dipole coupling, the tunnelling resistance becomes maximum at zero field. The ultrathin FeCo layer sandwiched between the Au and MgO layers exhibits considerable PMA (ref. 16). Therefore, its magnetization was easily saturated in the perpendicular direction by a relatively small perpendicular magnetic field of approximately 1,500 Oe (Fig. 1a). As this saturation field reflects the PMA of the ultrathin FeCo layer, it should be controlled by voltage application. Figure 1b shows the bias voltage dependence of the MR curves under the perpendicular field, where the vertical axis is normalized

[1]Graduate School of Engineering Science, Osaka University, Toyonaka, Osaka, 560-8531, Japan, [2]CREST, Japan Science Technology Agency, 4-1-8 Honcho, Kawaguchi, Saitama, 3323-0012, Japan. †Present address: Spintronics Research Center, AIST, Tsukuba, Ibaraki, 305-8568, Japan.
*e-mail: suzuki-y@mp.es.osaka-u.ac.jp.

© 2012 Macmillan Publishers Limited. All rights reserved

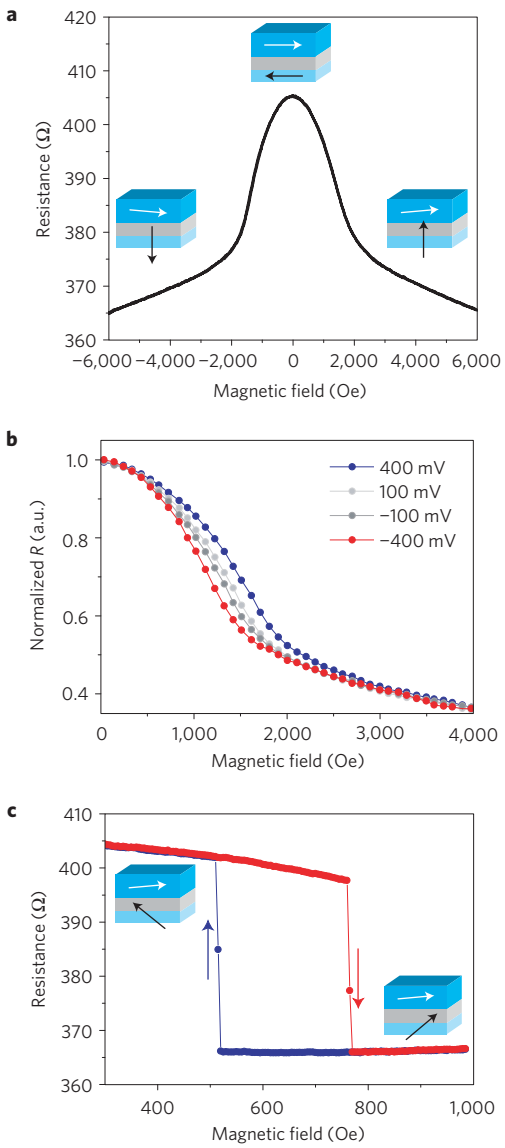

Figure 1 | Tunnelling magnetoresistance and voltage-induced anisotropy change in an ultrathin FeCo (001)/MgO (001)/Fe (001) junction. **a**, Magnetoresistance (MR) curve under a magnetic field perpendicular to the film plane. **b**, Bias voltage dependence of normalized MR curves under a magnetic field perpendicular to the film plane. **c**, MR hysteresis curve under an external field, tilted at an angle of 6° from the film's normal direction towards an in-plane easy axis of the rectangularly shaped FeCo ultrathin magnetic cell (see illustration in Fig. 3a). The hysteresis represents abrupt switching in the in-plane component of the magnetization in the ultrathin FeCo layer. White and black arrows in **a** and **c** indicate the magnetization of the top Fe layer and the bottom ultrathin FeCo layer respectively.

by the maximum ($H_{ex} = 0$ Oe) and minimum ($H_{ex} = 18$ kOe) resistance to compare the shape of the curves. A change in the saturation field of approximately 400 Oe was induced by bias voltage applications of ±400 mV. The saturation field becomes smaller (larger) for negative (positive) voltages. The amplitude of the anisotropy field change and its sign are almost identical to those in our previous study[22]. The PMA in this sample can be modulated by an applied voltage (for details, see Supplementary Information). For the coherent switching experiment, an external magnetic field was applied at a tilt angle of 6° from the film's normal direction towards the in-plane easy axis. The external field raises the magnetization from the film plane by around 45° and maximizes the anisotropy torque. The in-plane component of the external field causes an abrupt switching of the in-plane component of the magnetization, and a square hysteresis appears in the MR curve (see the minor MR curve in Fig. 1c).

We first performed a macro-spin model simulation based on the conventional Landau–Lifshitz–Gilbert (LLG) equation for a cosine vector of magnetization $\mathbf{m} = (m_x, m_y, m_z)$ where the value of the damping constant, α was 0.01 (ref. 6). The effective field $\mathbf{H}_{eff}$, which is obtained from the magnetic anisotropy energies and the Zeeman energy, is expressed as follows:

$$\mathbf{H}_{eff} = -\nabla_m \left[\frac{1}{2} \left(H_c m_y^2 + H_{s,perp}(V) m_z^2 \right) - \mathbf{m} \cdot \left(\mathbf{H}_{ext} + \mathbf{H}_{dipole} \right) \right]$$

Here, the appropriate values of the in-plane coercive field, H_c (= 25 Oe) and the in-plane dipole field, H_{dipole} (= 73 Oe) exerted by the reference layer, are used in the calculation. The voltage effect is introduced as the change in the perpendicular anisotropy field $H_{s,perp}$, which is assumed to be 1,400 Oe under a zero electric field and 600 Oe under a pulse electric field of -1.0 V nm^{-1} (these values were obtained from the linear extrapolation in Supplementary Fig. S1b). The external field was set to 700 Oe at a tilt angle of 6° from the film's normal direction. We used a voltage pulse with rise and fall times of 70 ps (Fig. 2a); this is identical to our experimental conditions. Figure 2b shows examples of the calculated trajectories for various durations (τ_{pulse}). The influence of temperature is omitted here ($T = 0$ K). The initial and final magnetization states are denoted by I.S. and F.S., respectively, and the red (blue) line indicates the trajectory during the pulse application (after the pulse is turned off—the relaxation process). The final state is stabilized to the identical or the reversed position with respect to the initial state, depending on τ_{pulse}. For example, the magnetization can be switched by 180° when $\tau_{pulse} = 0.4$ ns, while it is switched back to the initial state by rotation through an angle of 360° when $\tau_{pulse} = 0.8$ ns. As for the relaxation process, the precession angle becomes larger for longer pulse durations. From these observations, we predict that the switching probability should oscillate depending on τ_{pulse} and become smaller for the longer pulse duration, because a large precession angle may be susceptible to the effect of thermal magnetization fluctuation at room temperature.

The experimental arrangement to measure coherent magnetization switching is shown in Fig. 3a. A voltage pulse with fast rise and fall times of 70 ps was applied by a pulse generator (Picosecond Pulse Labs; Model 10,070A) to the MTJ through an attenuator (−3 dB) and an RF port of the bias tee. The duration time τ_{pulse} was varied from 0.25 to 8.15 ns. The magnetization switching of the free layer was monitored by resistance measurements using a lock-in amplifier through a d.c. port of the bias tee. A tilted external magnetic field H_{ext} was applied in the field range of the bistable magnetization state of the FeCo free layer (530–730 Oe, see Fig. 1c).

Figure 3b,c shows the tunnelling resistance measured after 50 successive negative and positive pulse voltage applications. The magnetization state was initialized to AP for the results seen in Fig. 3b. The magnetization states were not initialized after each pulse application. For a negative voltage pulse of −0.76 V with $\tau_{pulse} = 0.55$ ns (Fig. 3b), switching between the P and AP states was observed in almost all pulse applications. On the other hand, for a positive voltage pulse of +0.76 V, no switching event was observed regardless of the initial magnetization configuration (results for both P and AP cases are shown in Fig. 3c). This is because the voltage effect in the positive bias direction cannot excite coherent switching, owing to the suppression of the PMA. Here, the pulse electric field penetrating the MgO insulating layer was estimated to be approximately ±1.0 V nm^{-1} by considering the reflected voltage pulse caused by the impedance mismatch.

© 2012 Macmillan Publishers Limited. All rights reserved

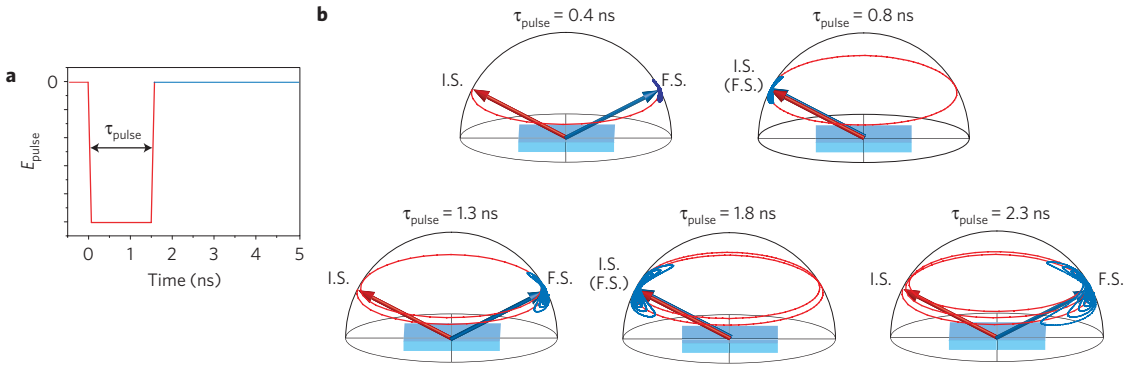

Figure 2 | Macro-spin model simulation of coherent magnetization switching under various pulse duration conditions. a, Shape of the applied voltage pulse used in the simulation. Pulse durations, τ_{pulse}, are full-widths at half-maximum with rise and fall times of 70 ps. **b**, Examples of calculated trajectories induced by voltage pulse application. Initial state (I.S.) and final state (F.S.) represent the magnetization state before and after pulse voltage application.

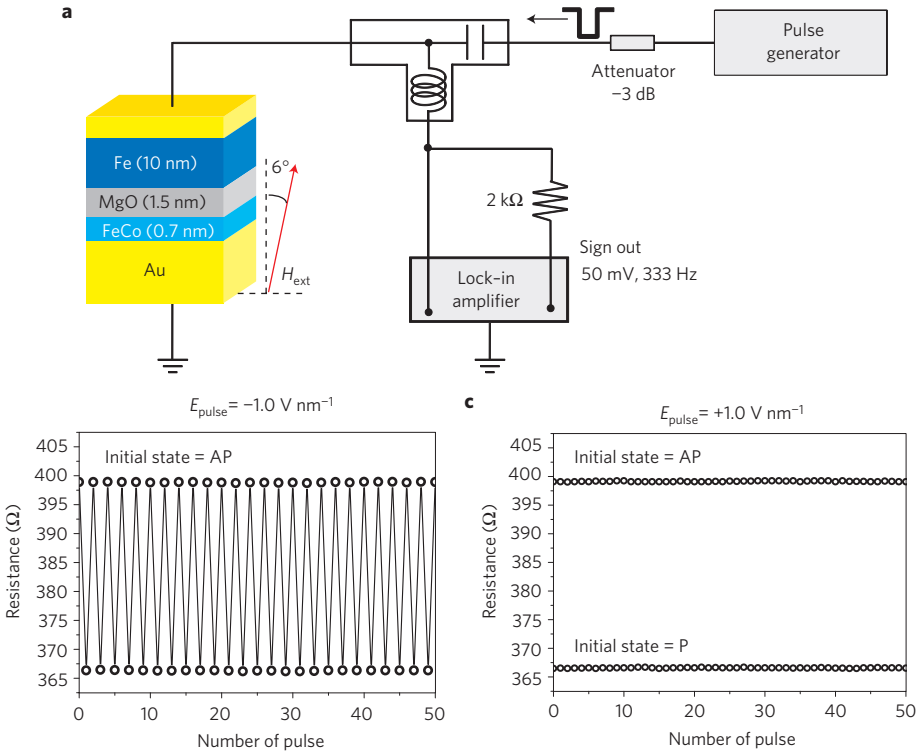

Figure 3 | Pulse-voltage-induced coherent magnetization switching. a, Schematic of the measurement set-up and sample structure of the MTJ device. Voltage pulses were applied to the MTJ using a pulse generator and the a.c. resistance of the sample was monitored using a standard lock-in technique. **b**,**c**, Examples of magnetization switching events induced by 50 successive pulse voltage applications. The amplitudes of the applied electric field are $E_{pulse} = -1.0$ V nm^{-1} in **b** and $E_{pulse} = +1.0$ V nm^{-1} in **c**. The external magnetic field H_{ext} and pulse duration τ_{pulse} are 700 Oe and 0.55 ns, respectively. The initial magnetization state is AP for experiment **b** and the magnetization condition is not initialized after each pulse voltage application. For **c**, results for both P and AP initial conditions are shown. No switching events were observed in this electric field polarity.

Detailed analyses of the switching probability P_{switch} for the negative voltage case were carried out. Figure 4a,b shows the P_{switch} diagram for AP to P and P to AP switching as functions of τ_{pulse} and H_{ext}, respectively. Surprisingly, a clear oscillation of P_{switch} was observed depending on the value of τ_{pulse}. Furthermore, P_{switch} is higher in the short τ_{pulse} region (of the order of sub-nanoseconds). To understand the observed oscillatory behaviour, we calculated P_{switch} using the macro-spin model simulation discussed above. The influence of room temperature (T = 300 K) was introduced as the effective thermal fluctuation field ($= \sqrt{\{2k_B T\alpha / V_{cell} M_s \gamma (1+\alpha^2)\Delta t\}}$; ref. 26) with an isotropic 3D Gaussian distribution. The terms $\mu_0 M_s$ (= 1.54 T), k_B (= 1.38×10^{-23} J K^{-1}), V_{cell} (= 1.12×10^{-22} m^3) and Δt (= 0.5 ps) denote the saturation magnetization, the Boltzmann constant, the volume of the calculation cell and the duration of the constant effective thermal fluctuation field, respectively. The values of H_c, H_{dipole} and $H_{s,perp}$, including the electric field effect, are identical to those in the calculation used for Fig. 2b. The calculation results for AP to P switching are shown in Fig. 4c; Fig. 4d shows the calculation results for P to AP switching. The oscillation period and phase were reproduced completely.

Because a finite tunnelling current flows in the MTJ, we need to consider its influence on the magnetization switching—for example, the influence of current-induced magnetic field and the spin-transfer effect. The maximum applied current is −3.8 mA; this corresponds to a current density of -2.4×10^{10} A m^{-2} in this

© 2012 Macmillan Publishers Limited. All rights reserved

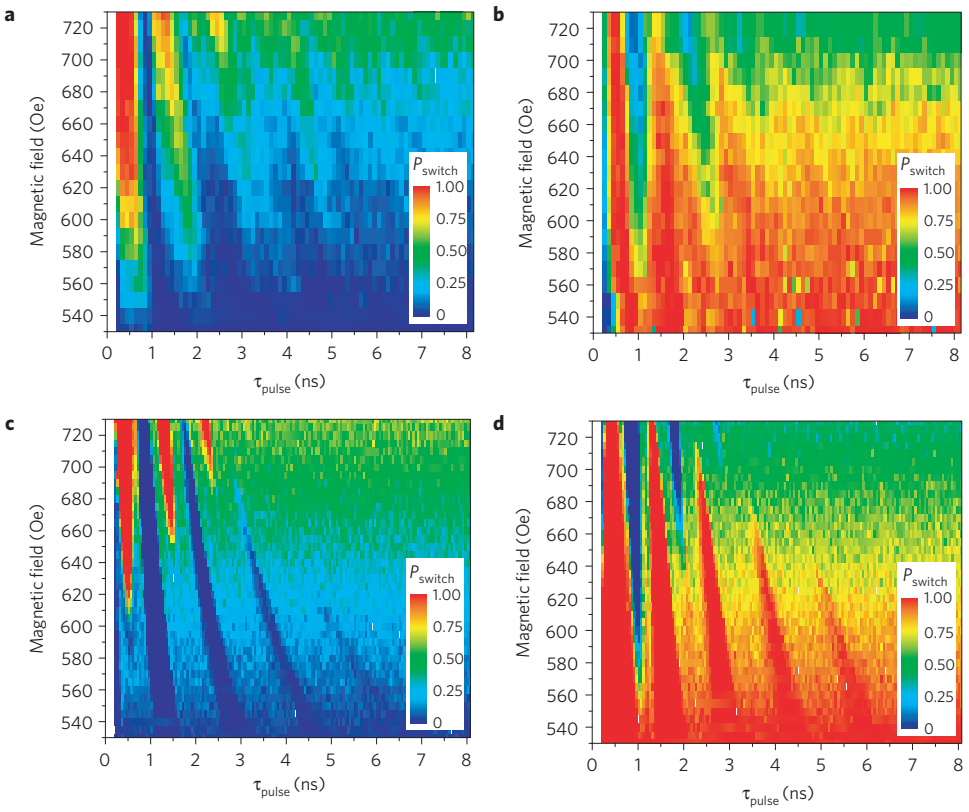

Figure 4 | Switching probability (P_{switch}) diagram as functions of pulse duration time τ_{pulse} and external magnetic field. a,**b**, Experimental results under $E_{pulse} = -1.0$ V nm^{-1}. **c**,**d**, Calculated results using macro-spin model simulation. Switching events from AP to P and P to AP states are shown in **a**,**c** and **b**,**d**, respectively. For the simulation, a voltage-induced anisotropy change was included as the effective field change in the perpendicular direction; $H_{s,perp}(0\ \text{V nm}^{-1}) = 1,400$ Oe and $H_{s,perp}(-1.0\ \text{V nm}^{-1}) = 600$ Oe. The measurements and calculations were repeated 100 times in each pixel; the red (blue) region represents high (low) P_{switch}.

experiment. From the qualitative perspective, as the spin-transfer torque is an anti-damping (damping) torque for the negative (positive) applied pulse in the AP state, it may cause a switch from the AP to the P state; however, a switch from P to AP cannot occur without a change in the polarity of the pulses. Therefore, we can certainly exclude spin-transfer switching in our experiment, in which two-way toggle switching was realized by employing electric pulses with unique polarity (Fig. 3b). From the quantitative perspective, the torque introduced by the voltage is approximately 67 times that of the current-induced magnetic field and approximately 68 times that of spin-transfer; the influence of this torque is dominant over the other two effects (for details, see Supplementary Information) and we conclude that only the voltage-induced excitation of the magnetization dynamics can explain the observed results.

As the experiments were done using coaxial cables and waveguides, the energy needed to reverse the magnetization was determined by their charging energies. However, the energy absorbed by the junction should ideally be determined by the capacitance of the junction if the resistance of the junction is large enough. The estimated charging energy of the target junction with a lateral size of 50 nm under a voltage of 0.76 V is approximately 10,000 $k_B T$; further, this value is approximately 1/500th of that required for spin-transfer switching.

By applying a short voltage pulse, of the order of sub-nanoseconds, in a MTJ with an ultrathin ferromagnetic metal film, we realized coherent magnetization switching under a constant bias magnetic field. The toggle switching between the P and AP magnetization states was controlled by the pulse duration time. It is noteworthy that by controlling the voltage pulse shape with the fast rise and slow fall times (as suggested in our previous work[6]) we can realize coherent switching with a high tolerance to pulse duration time. We believe that our results have a significant technological impact and our approach provides a new method for magnetization switching in voltage-driven spintronics devices.

Received 25 May 2011; accepted 14 October 2011; published online 13 November 2011

References

1. Berger, L. Emission of spin waves by a magnetic multilayer traversed by a current. *Phys. Rev. B* **54,** 9353–9358 (1996).
2. Slonczewski, J. C. Current-driven excitation of magnetic multilayers. *J. Magn. Magn. Mater.* **159,** L1–L7 (1996).
3. Curie, P. Sur la symétrie dans les phénomènes physiques, symétrie d'un champ électrique et d'un champ magnétique. *J. Phys.* **3,** 393–415 (1894).
4. Nie, X. & Blügel, S. Elektrisches Feld zur Ummagnetisierung eines dünnen Films. European patent 19841034.4 (2000).
5. Weisheit, M. *et al.* Electric field-induced modification of magnetism in thin-film ferromagnets. *Science* **315,** 349–351 (2007).
6. Maruyama, T. *et al.* Large voltage-induced magnetic anisotropy change in a few atomic layers of iron. *Nature Nanotech.* **4,** 158–161 (2009).
7. Gamble, S. J. *et al.* Electric field induced magnetic anisotropy in a ferromagnet. *Phys. Rev. Lett.* **102,** 217201 (2009).
8. Gerhard, L. *et al.* Magnetoelectric coupling at metal surfaces. *Nature Nanotech.* **5,** 792–797 (2010).
9. Novosad, V. *et al.* Novel magnetostrictive memory device. *J. Appl. Phys.* **87,** 6400–6402 (2000).
10. Lee, J-W., Shin, S-C. & Kim, S-K. Spin engineering of CoPd alloy films via the inverse piezoelectric effect. *Appl. Phys. Lett.* **82,** 2458–2460 (2003).
11. Ohno, H. *et al.* Electric-field control of ferromagnetism. *Nature* **408,** 944–946 (2000).
12. Chiba, D., Yamanouchi, M., Matsukura, F. & Ohno, H. Electrical manipulation of magnetization reversal in a ferromagnetic semiconductor. *Science* **301,** 943–945 (2003).

© 2012 Macmillan Publishers Limited. All rights reserved

13. Chiba, D. *et al.* Magnetization vector manipulation by electric fields. *Nature* **455,** 515–518 (2008).
14. Eerenstein, W., Mathur, N. D. & Scott, J. F. Multiferroic and magnetoelectric materials. *Nature* **442,** 759–765 (2006).
15. Chu, Y-H. *et al.* Electric-field control of local ferromagnetism using a magnetoelectric multiferroic. *Nature Mater.* **7,** 478–482 (2008).
16. Shiota, Y. *et al.* Voltage-assisted magnetization switching in ultrathin $Fe_{80}Co_{20}$ alloy layers. *Appl. Phys. Express* **2,** 063001 (2009).
17. Endo, M., Kanai, S., Ikeda, S., Matsukura, F. & Ohno, H. Electric-field effects on thickness dependent magnetic anisotropy of sputtered $MgO/Co_{40}Fe_{40}B_{20}/Ta$ structures. *Appl. Phys. Lett.* **96,** 212503 (2010).
18. Duan, C-G. *et al.* Surface magnetoelectric effect in ferromagnetic metal films. *Phys. Rev. Lett.* **101,** 137201 (2008).
19. Nakamura, K. *et al.* Giant modification of the magnetocrystalline anisotropy in transition-metal monolayers by an external electric field. *Phys. Rev. Lett.* **102,** 187201 (2009).
20. Tsujikawa, M. & Oda, T. Finite electric field effects in the large perpendicular magnetic anisotropy surface Pt/Fe/Pt(001): A first-principles study. *Phys. Rev. Lett.* **102,** 247203 (2009).
21. Nozaki, T., Shiota, Y., Shiraishi, M., Shinjo, T. & Suzuki, Y. Voltage-induced perpendicular magnetic anisotropy change in magnetic tunnel junctions. *Appl. Phys. Lett.* **96,** 022506 (2010).
22. Shiota, Y. *et al.* Quantitative evaluation of voltage-induced magnetic anisotropy change by magnetoresistance measurement. *Appl. Phys. Express* **4,** 043005 (2011).
23. Yuasa, S., Nagahama, T., Fukushima, A., Suzuki, Y. & Ando, K. Giant room-temperature magnetoresistance in single-crystal Fe/MgO/Fe magnetic tunnel junctions. *Nature Mater.* **3,** 868–871 (2004).
24. Parkin, S. S. P. *et al.* Giant tunnelling magnetoresistance at room temperature with MgO(100) tunnel barriers. *Nature Mater.* **3,** 862–867 (2004).
25. Chiba, D., Nakatani, Y., Matsukura, F. & Ohno, H. Simulation of magnetization switching by electric-field manipulation of magnetic anisotropy. *Appl. Phys. Lett.* **96,** 192506 (2010).
26. Akimoto, H., Kanai, H., Uehara, Y., Ishizuka, T. & Kameyama, S. Analysis of thermal magnetic noise in spin-valve GMR heads by using micromagnetic simulation. *J. Appl. Phys.* **97,** 10N705 (2005).

Acknowledgements

We would like to thank H. Tomita for his help with the simulations as well as S. Miwa for useful discussions. Y. Shiota thanks the Japan Society for the Promotion of Science for the fellowship. Part of this research was conducted under the financial support of the Global Center of Excellence (G-COE) program of the Ministry of Education, Culture, Sports, Science and Technology, Japan (MEXT).

Author contributions

Y. Suzuki conceived and designed the experiments. Y. Shiota performed the experiments, simulations, and analysis. T.N. and Y. Suzuki led experiments and physical discussions. F.B., S.M., and T.S. contributed to the general discussions. Y. Shiota wrote the paper with reviews and inputs from Y. Suzuki and T.N.

Additional information

The authors declare no competing financial interests. Supplementary information accompanies this paper on www.nature.com/naturematerials. Reprints and permissions information is available online at http://www.nature.com/reprints. Correspondence and requests for materials should be addressed to Y.Suzuki

© 2012 Macmillan Publishers Limited. All rights reserved